Journal of Power Sources 252 (2014) 270–276

Contents lists available at ScienceDirect

Journal of Power Sources

journal homepage: www.elsevier.com/locate/jpowsour

Phosphoric acid doped polybenzimidazole/imidazolium-modified silsesquioxane hybrid proton conducting membranes for anhydrous proton exchange membrane application

Bencai Lin [a,b], Fuqiang Chu [a], Ningyi Yuan [a,b,*], Hui Shang [a], Yurong Ren [a], Zongzong Gu [a], Jianning Ding [a,b,*], Yingqiang Wei [a], Xiaomin Yu [a]

[a] Center for Low-Dimensional Materials, Micro-Nano Devices and Systems, Jiangsu Key Laboratory for Solar Cell Materials and Technology, Changzhou University, Changzhou 213164, Jiangsu, China
[b] Jiangsu Collaborative Innovation Center of Photovolatic Science and Engineering, Changzhou 213164, Jiangsu, China

HIGHLIGHTS

- Addition of Im-$SiO_{3/2}$ dramatically increased the H_3PO_4 doping capacity of the membranes.
- The PA-doped hybrid membranes show the conductivity of 6.3×10^{-2} S cm^{-1} at 180 °C.
- Im-$SiO_{3/2}$ is effective in preventing the release of H_3PO_4 from the hybrid membranes.

ARTICLE INFO

Article history:
Received 4 September 2013
Received in revised form
26 November 2013
Accepted 26 November 2013
Available online 6 December 2013

Keywords:
Polymer electrolyte membrane
Hybrid membrane
Fuel cells
Sol–gel
Inorganic additives

ABSTRACT

Phosphoric acid doped polybenzimidazole (PBI)/imidazolium-modified silsesquioxane (Im-$SiO_{3/2}$) hybrid membranes with high proton conductivity at high temperature under anhydrous conditions are synthesized and characterized. The presence of Im-$SiO_{3/2}$ is confirmed by FT-IR and energy-dispersive X-ray spectroscopy (EDS) mapping of silicon element. The phosphoric acid uptake and proton conductivity of the hybrid membranes increase with the Im-$SiO_{3/2}$ content, and the conductivity of PBI/Im-$SiO_{3/2}$-20 reaching 6.3×10^{-2} S cm^{-1} at 180 °C. Compared with pure PBI membranes, the introduction of Im-$SiO_{3/2}$ is effective in preventing the release of the phosphoric acid component from the hybrid membranes. The properties of the prepared hybrid membranes indicate their promising prospects in anhydrous proton exchange membrane applications.

1. Introduction

Polymer electrolyte membrane fuel cells (PEMFCs) are promising electrochemical devices which could provide clean and efficient energy for stationary, transportation and portable electronics [1]. As one of the key components of PEMFCs, proton exchange membrane (PEM) acts both as an electrolyte to transport protons from the anode to the cathode and a barrier to fuel crossover between the electrodes. As commercially available PEMs, perfluorosulfonic acid membranes, such as Nafion, have been widely studied due to their high proton conductivity, excellent chemical and mechanical properties [2]. However, they cannot be used at temperatures above 80 °C due to the rapid loss of conductivity which resulted by the evaporation of water [3,4]. The operation of PEMFCs at elevated temperature could improve electrode kinetics at both electrodes, enhance the CO tolerance of the platinum catalyst at the anode, and simplify heat and water managements of PEMFCs [5,6]. Therefore, it is desirable to develop alternative PEMs with high thermal stability and satisfactory proton conductivity at elevated temperature under anhydrous conditions.

Recently, many studies have been carried out to develop new or modified commercially polymer electrolyte membranes with good fuel cell performance above 80 °C [7–13]. Among the various types of polymers have been reported, polybenzimidazole (PBI) has been recognized as a good choice for preparation of PEMs for high temperature PEMFC because of its excellent chemical stability, good

* Corresponding authors. Jiangsu Collaborative Innovation Center of Photovolatic Science and Engineering, Changzhou 213164, Jiangsu, China. Tel./fax: +86 519 86450008.
E-mail addresses: nyyuan@cczu.edu.cn (N. Yuan), dingjn@cczu.edu.cn (J. Ding).

0378-7753/$ – see front matter © 2013 Elsevier B.V. All rights reserved.
http://dx.doi.org/10.1016/j.jpowsour.2013.11.102

thermochemical and mechanical stabilities [12,13]. However, the proton conductivity of PBI should be enhanced because its low proton conducting ability. Sulfonated polymers with the sulfonic acid groups have become an important approach in enhancing proton conductivity of the PEMs [14]. A high degree of sulfonation improves the proton conductivity, whereas lead to a high swelling ratio which result in the loss of the mechanical strength and the increase of fuel permeability [15]. The incorporation of hydrophilic/hygroscopic inorganic additives, such as silica [16,17] and titanium dioxide [18,19] into the sulfonated polymer membrane matrix is a common approach to enhance the conductivity of PEMs. In addition, incorporation of inorganic additives could also improve the mechanical stability of membranes [11]. However, this type of hybrid PEMs can hardly retain water and maintain high conductivity above 130 °C [20].

Replacement of water with low-volatile proton carrier (such as phosphoric acid or proton ionic liquids) is another simple and powerful method to improve the proton conductivity of PEMs especially at high temperature [21–24]. Among the various types of PEMs, phosphoric acid (PA) doped PBI have been attracted much attention because of their high conductivities at elevated temperature [25]. PA can generate both proton donor (acidic) and proton acceptor (basic) groups, and protons can readily transfer by the dynamic hydrogen bond networks formed by phosphoric acid inside the membranes [26–28]. In addition, the incorporation of PA could increase water uptake which favors the proton conductivity of PEMs [29], and the proton conductivity of the PA doped membranes strongly depends on the PA doping level. However, a high acid doping level often decreases the mechanical and chemical stability of the membranes, especially at elevated temperature [30]. Moreover, the performance of fuel cells could be affected by the release of the phosphoric acid from PEMs. Recently, several approaches, including synthesis of new types of ionic polymers [31] and incorporation of inorganic fillers into the polymeric matrix [13] to enhance the PA retention, have been pursued to obtain PEMs with high conductivity at elevated temperature under anhydrous conditions. Yan and coworkers [13] synthesized PBI/H_3PO_4/zwitterion-coated silica (ZC-SiO_2) hybrid membranes, the addition of ZC-SiO_2 to the PBI membrane dramatically increased the phosphoric acid doping capacity, and slightly improved the chemical stability of the hybrid membranes. In addition, ZC-SiO_2 are effective in preventing the release of phosphoric acid component from the hybrid membranes.

In the present work, a new type of PBI-based hybrid PEMs for potential application in high temperature PEMFCs will be prepared via a sol–gel process from PBI and an organic silicon source, *N*-(3-propyltrimethoxysilane)imidazole (PTMSIm), and then doped with phosphoric acid after casting film. Imidazole functionalized inorganic networks or imidazolium-modified silsesquioxane (Im-$SiO_{3/2}$) could be formed for the hydrolysis of PTMSIm. It is expected that the inorganic networks or Im-$SiO_{3/2}$ of the membranes offers good mechanical strength, while the imidazole groups improve the phosphoric acid uptake ability. The properties of the membrane can be adjusted by adjusting the content of PTMSIm. The influence of PTMSIm content on the hybrid membrane properties was systematically investigated with respect to their thermal stability, mechanical property, microstructure and proton conductivity. In addition, the effect of the PTMSIm in preventing the release of phosphoric acid was also studied.

2. Experimental

2.1. Materials

Imidazole, γ-chloropropyltrimethoxysilane, sodium ethoxide, 2,2-bis (4-carboxyphenyl) hexafluoropropane, 3,3′-diaminobenzidine, poly(phosphoric acid), phosphoric acid, methanol, *N*,*N*-dimethylaceramide (DMAc), dimethylsulfoxide (DMSO). In all experiments distilled deionized water was used.

2.2. Synthesis of N-(3-propyltrimethoxysilane) imidazole (PTMSIm)

The sol–gel precursor PTMSIm was synthesized as documented in previous literature [32]. Briefly, 3.40 g sodium ethoxide (0.05 mol) 3.40 g imidazole (0.05 mol) were dissolved in100 mL methanol under stirring at 0 °C. Then 9.94 g (0.05 mol) of γ-chloropropyltrimethoxysilane was added and the mixture was stirred at reflux for 24 h under nitrogen. The suspension was filtered off and the solvent was removed under dynamic vacuum. The product PTMSIm is a non-viscous liquid. ^{1}H NMR (250 MHz, $CDCl_3$): δ: 7.54 (s, 1H); 7.01 (s, 1H); 6.88 (s, 1H); 3.88 (t, 2H); 3.53 (s, 9H); 1.83 (q, 2H); 0.54 (t, 2H).

2.3. Preparation of PBI

Fluorine-containing PBI was synthesized via the condensation polymerization of 3,3-diaminobenzidine and 2-bis(4-carboxyphenyl) hexafluoropropane in PPA at 170 °C, following the synthetic procedure reported in literature [13].

2.4. Preparation of composite membranes

PBI-based hybrid membranes were prepared as follows: a mixture containing 2 wt% PBI in DMAc solution and a certain amount of PTMSIm was vigorously stirred for 0.5 h at room temperature to form a homogeneous solution. Subsequently, hydrochloric acid was added into the solution in a dropwise manner until pH = 2. The mixed solution was vigorously stirred for 6 h under nitrogen atmosphere. Then the solution was cast onto a glass plate with a doctor's knife, and dried in a vacuum at 70 °C for 24 h to remove the solvent slowly. Finally, a free-standing yellow transparent membrane with a thickness of approximately 50 μm was obtained.

2.5. Phosphoric acid-doping level

The prepared PBI-based hybrid membranes were doped with phosphoric acid by immersing them in a phosphoric acid aqueous solution (85 wt%) for one week at room temperature. To exclude the weight gain due to the water uptake, the doped membranes were dried at 110 °C under vacuum until the membrane weights unchanged with time. The phosphoric acid doping level is defined as the weight change after and before dipping in phosphoric acid solution and can be calculated using the following equation:

$$W(\%) = \frac{(W_W - W_d)}{W_d} \times 100\%$$

where W_w and W_d are membrane weights after and before dipping in phosphoric acid solution, respectively.

2.6. Characterizations

^{1}HNMR spectra were recorded on a Varian 250 MHz spectrometer. Fourier transform infrared (FT-IR) spectra of the polymers were recorded on a Varian CP-3800 spectro-meter in the range of 4000–400 cm^{-1}. Thermal analysis was carried out by Universal Analysis 2000 thermogravimetric analyzer (TGA). Samples were heated from 30 to 700 °C at a heating rate of 10 °C min^{-1} under a nitrogen flow. Scanning electron microscopy (SEM) images were taken with a Hitachi S-4800 microscope with an accelerating

voltage of 15 kV. The tensile properties of membranes were measured by using an Instron 3365 at 30 °C at a crosshead speed of 5 mm min^{-1}.

2.7. Proton conductivity

The resistance of the PBI-based composite membranes was measured by the AC impedance method over the frequency range 1 Hz to 1 MHz using electrochemical workstations (Zahner IM6EX). The membranes were dried at 100 °C for 8 h under a vacuum before the conductivity measurement to remove water from the membranes. A rectangular piece of dry membrane was sandwiched between two gold electrodes in a glass cell which was placed in the head space of a temperature controlled vessel [13], and the conductivity of membranes was measured in a dry nitrogen atmosphere. Before the measurements at each temperature set point, the samples were held at constant temperature for at least 10 min.

3. Results and discussion

3.1. Preparation of hybrid membranes

It has been demonstrated that fluorine-containing PBI shows better processability and oxidative-stability than that of other PBIs [33,34]. Therefore, fluorine-containing PBI was chosen as a polymer matrix for the preparation of hybrid membranes. The preparation of PBI-based hybrid membranes was shown in Scheme 1. As an organic silicon source, the hydrolysis of PTMSIm at the presence of acid could form imidazolium functionalized silsesquioxane (Im-$SiO_{3/2}$). The PBI-based hybrid membranes were prepared by dissolving PBI and PTMSIm in DMAc followed by casting on a glass plate. The produced hybrid membranes are coded as PBI/Im-$SiO_{3/2}$-X, where X denotes the weight percentage of PTMSIm in the hybrid membranes.

3.2. FT-IR spectra

Fig. 1 shows the FT-IR spectra of pure PBI (Fig. 1A), PTMSIm (Fig. 1B) and PBI/Im-$SiO_{3/2}$-20 hybrid membranes (Fig. 1C), respectively. The broad absorption band at approximately 3000–3500 cm^{-1} is assigned to N–H absorption and stretching vibrations of self-associated hydrogen-bonded N–H···N groups in Fig. 1A [13]. The absorption bands at about 1631, 1260 and 810 cm^{-1} represent the stretching vibration of C=N groups and the absorption of the benzene ring, respectively, which are the characteristic peaks of PBI. Fig. 1B shows the FT-IR spectrum of PTMSIm, the absorption bands present at about 2970 cm^{-1} corresponds to the stretching of methylene and methyl, and the presence of absorption bands at about 770 cm^{-1} and 1110 cm^{-1} is related to the vibration of Si–O and Si–O–C, the absorption band at about 1600 cm^{-1} and 1570 cm^{-1} is related to C=N and C=C vibrations of imidazole ring. Compared with the pure PBI membrane, the hybrid membrane shows new absorption peaks at 2962, 1576 and 1114 cm^{-1} which are the characteristic peaks of PTMSIm. These results demonstrate the existence of Im-$SiO_{3/2}$ in the hybrid membrane.

3.3. SEM and EDS

Scanning electron microscopy (SEM) and a spectrum obtained by mapping with energy dispersive spectroscopy (EDS) provided information about the surface view, cross-sectional view and the elemental composition of the membrane on a micrometer scale. Fig. 2A and B shows surface morphology of the pure PBI membranes and PBI/Im-$SiO_{3/2}$. From the SEM images, it can be clearly seen that the pure PBI membrane surface is smooth. Compare with the pure PBI membrane, little mounds were observed in the SEM images of PBI/Im-$SiO_{3/2}$-20 which are related to Im-$SiO_{3/2}$ formed by the hydrolysis of PTMSIm. The cross-section view of PBI/Im-$SiO_{3/2}$-20 (Fig. 2D) showed that the resultant membranes are uniform, compact, and without any visible pores in the interior of the membranes. The presence of silicon element is confirmed by EDS maps of PBI/Im-$SiO_{3/2}$-20, which further confirming the existence of Im-$SiO_{3/2}$ in the hybrid membrane (Fig. 2C and E).

3.4. Thermal analysis

The thermal stability is a key property for PEMs operated at high temperatures, because work at high temperature could enhance the reaction kinetics at both electrodes and reduce the thermodynamic voltage losses of PEMFCs. The thermal properties of the PBI-based membranes were investigated by thermogravimetric analyzer (TGA), and the typical TGA curves of the phosphoric acid-doped membranes were showed in Fig. 3. With the temperature increased, three weight loss stages for all the composite membranes were observed. The weight loss of the first stage occurred at about 120 °C can be attributed to the evaporation of absorbed water

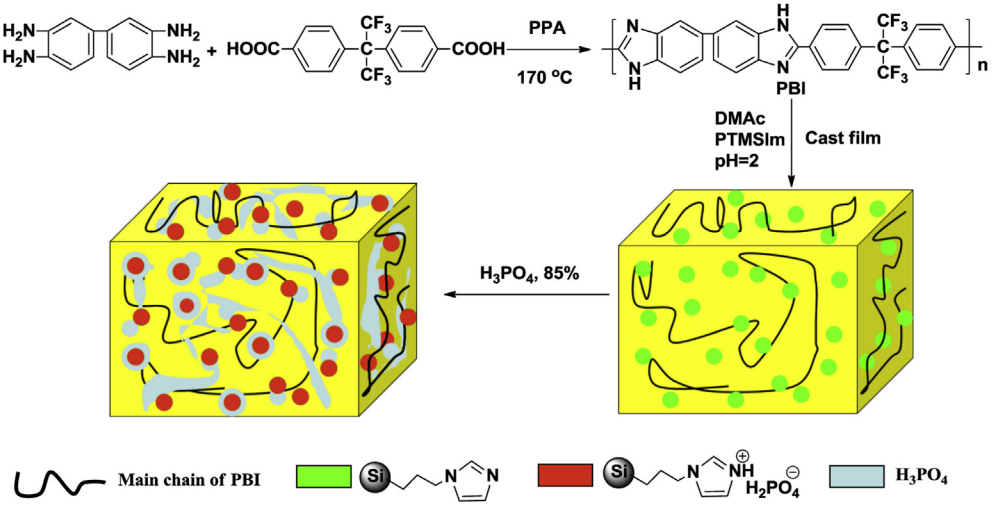

Scheme 1. Reaction scheme for the preparation of PBI-based hybrid membranes.

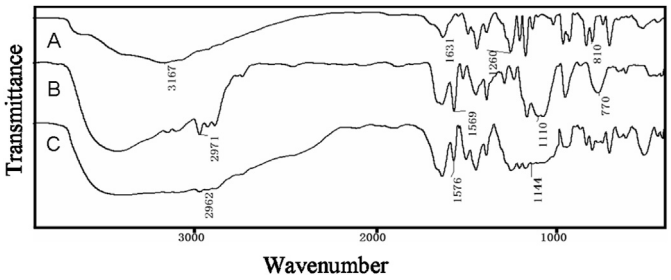

Fig. 1. FT-IR spectra of (A) pure PBI membrane, (B) PTMSIm and (C) PBI/Im-$SiO_{3/2}$-20 hybrid membrane.

and DMAc. The second weight loss temperature occurred at about 200–450 °C could be assigned to the decomposition of imidazole rings and H_3PO_4. The weight loss stage took place at about 550 °C was ascribed to the main-chain degradation of PBI. These results indicate that the membranes prepared in this work were thermally stable enough for the high temperature PEMFC application. The difference of thermal stability caused by the incorporation of Im-$SiO_{3/2}$ is negligible. Similar results have been observed for poly(styrene-co-acrylonitrile)/silica [11], PBI/H_3PO_4/ZC-SiO_2 [13] and sulfonated polymer/silica hybrid membranes [35]. This is probably due to the inorganic filler usually shows better thermally stable than polymers. The results of TGA indicated that the PBI-based hybrid membranes are stable enough for operation at elevated temperature (100–140 °C) for high temperature PEMFCs.

3.5. Mechanical properties

The mechanical stability is another key property for PEMs, and the effect of Im-$SiO_{3/2}$ content on the mechanical properties of the PBI-based hybrid membranes were studied with an Instron at room temperature. The measured tensile strength, Young's modulus and elongation at break of the H_3PO_4-doped and -undoped membranes are collected in Table 1. For the H_3PO_4-doped membranes, the pure PBI membrane showed a tensile strength of 56.33 MPa, a Young's modulus of 1350 MPa and an elongation at breaking of 28.13%. The tensile strength and Young's modulus increased with increasing the content of Im-$SiO_{3/2}$ in the hybrid membranes. For example, PBI/Im-$SiO_{3/2}$-5 showed a tensile strength of 58.31 MPa and a Young's

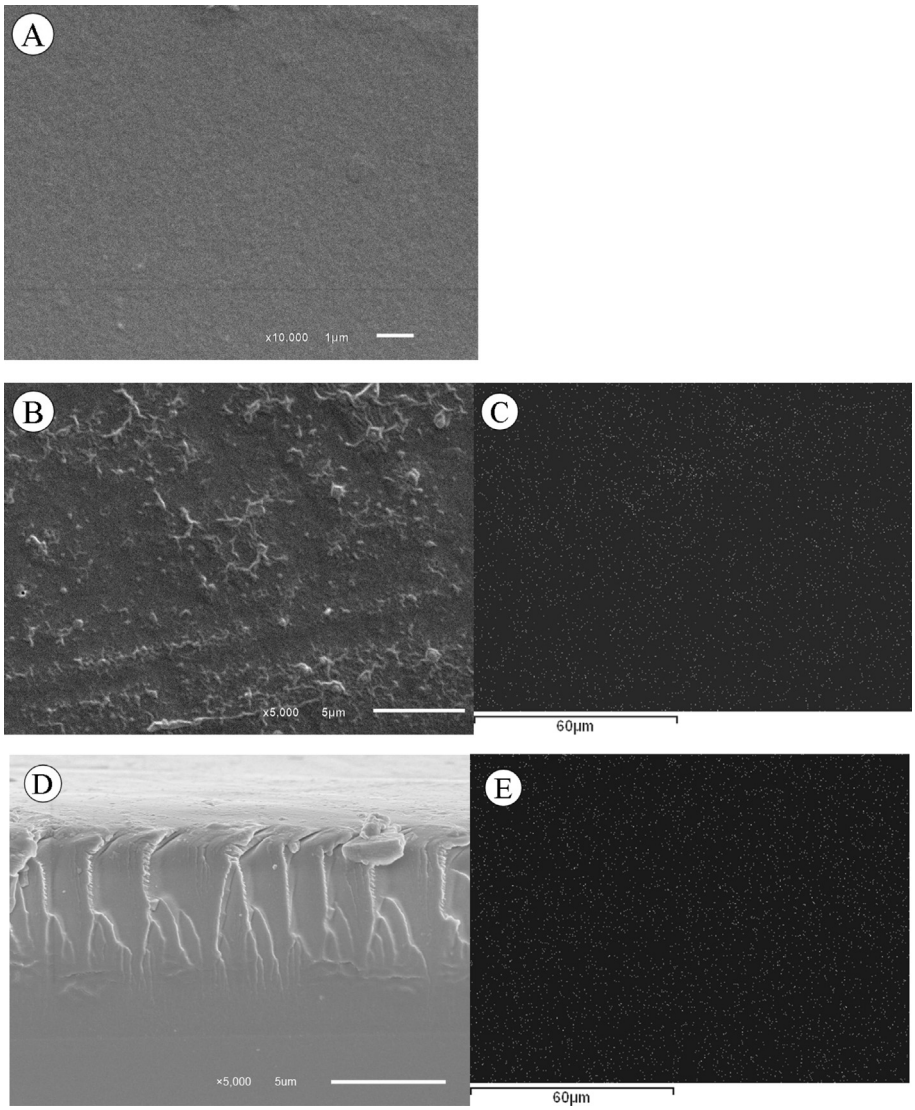

Fig. 2. SEM images of the surface of (A) pure PBI membrane, (B) PBI/Im-$SiO_{3/2}$-20 hybrid membrane, (C) distribution of silicon element in surface of PBI/Im-$SiO_{3/2}$-20 membranes, (D) the cross-sectional profiles of PBI/Im-$SiO_{3/2}$-20, and (E) distribution of silicon element in cross-sectional profiles of PBI/Im-$SiO_{3/2}$-20 membranes.

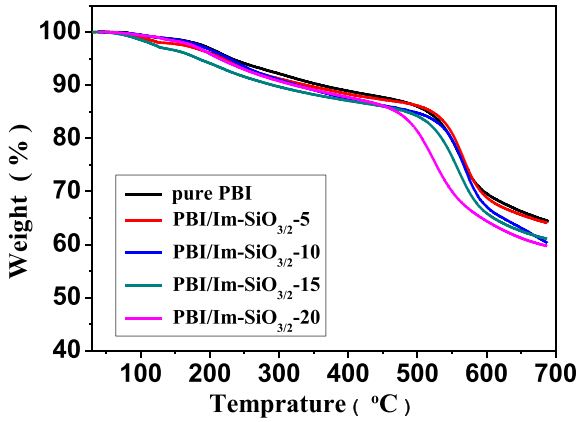

Fig. 3. Thermogravimetric analysis (TGA) curves of the phosphoric acid-doped membranes under nitrogen flow. Heating rate: 10 °C min^{-1}.

modulus of 1820 MPa, while the values reached 66.51 MPa and 2720 MPa for PBI/Im-$SiO_{3/2}$-20. However, the elongation at breaking of the hybrid membranes was decreased with the increasing of PTMSIm, and the elongation at breaking of PBI/Im-$SiO_{3/2}$-5 showed is 20.03%, the value decreased to 13.86% for PBI/Im-$SiO_{3/2}$-20 under the same conditions. For the acid-doped membranes, the doping H_3PO_4 reduced the tensile strength and Young's modulus but increased the elongation of the membranes. The tensile strength of all the doped membranes is in the range of 14.06–17.77 MPa, with a Young's modulus of 297–365 MPa, and elongation at break of 68–124%. After H_3PO_4 doping, the space of the PBI chains was increased which in turn reduces the intermolecular forces and consequently decreased the tensile strength and Young's modulus of the membranes [26]. Though PBI/Im-$SiO_{3/2}$-20 showed a much more H_3PO_4 uptake, it is worth noting that the tensile strength and Young's modulus of PBI/Im-$SiO_{3/2}$-20 was not lower than that of pure PBI membranes after H_3PO_4 doped. All these results indicated that the mechanical properties of PBI/Im-$SiO_{3/2}$-X membranes were improved by introducing Im-$SiO_{3/2}$.

3.6. H_3PO_4 doping level and proton conductivity

It has been demonstrated that the activation energy for the proton conduction is dependent on the acid doping ability as well as the relative humidity [26]. Therefore, the phosphoric acid doping ability is significantly important for PEMs, and the more doping mass of the phosphoric acid, the higher the conductivity of the PEMs. Here, the phosphoric acid doped PBI-based hybrid membranes were prepared, and the phosphoric acid doping ability of the PBI-based membranes is estimated by phosphoric acid uptake and summarized in Table 2. It should be noted that the phosphoric acid doping ability increases with the increase of the Im-$SiO_{3/2}$ content. For instance, the acid doping level of the pure PBI membrane was 108 wt%, which increased to 164 wt% for PBI/Im-$SiO_{3/2}$-20 (Table 2). The PBI/Im-$SiO_{3/2}$-X shows higher phosphoric acid uptake than that of PBI/H_3PO_4/ZC-SiO_2 hybrid membranes reported in previous work [13]. There are some reasons for the higher phosphoric acid uptake of hybrid membranes. Some phosphoric acid reacts with imidazole groups on the surface of Im-$SiO_{3/2}$ to form imidazolium salt, and the phosphoric acid uptake ability of the hybrid membrane was further improved by the interactions between the ionic groups of imidazolium salt and phosphoric acid [36]. In addition, the incorporated imidazolium groups could cause a separation of polymer backbones and created a more free volume for adopting phosphoric acid [26], which resulted in much more phosphoric acid uptake.

Proton conductivity is the most crucial property for a PEM. Fig. 4 shows the temperature-dependent proton conductivity of the PA-doped PBI-based membranes which were measured with an alternating current impedance spectroscopy in a closed cell under anhydrous conditions. As expected in all of the cases, the proton conductivity of the membranes increases with the temperature increase. For example, the conductivity of pure PBI membrane is about 5.4×10^{-3} S cm^{-1} at 100 °C, which increased to 2.9×10^{-2} S cm^{-1} at 180 °C. All the sample membranes show no decay in conductivity even at the temperature as high as 180 °C, which further indicating the excellent thermal stability of the PBI-based membranes.

Fig. 4 clearly showed that the proton conductivities of the PA-doped hybrid membranes are much higher than that of PA-doped pure PBI membranes. The pure PBI membrane shows the conductivity of 2.9×10^{-2} S cm^{-1} at 180 °C, while the value for PBI/Im-$SiO_{3/2}$-20 reaching 6.3×10^{-2} S cm^{-1} under the same experimental condition. There are two reasons for the higher conductivity of hybrid membranes: (i) more phosphoric acid uptake of the membranes; (ii) the inorganic component (Im-$SiO_{3/2}$) favors the formation of phosphoric acid continuous networks and interconnected channel in the hybrid membrane, and the proton conduction becomes more easy and feasible, compared to pure PBI membrane [11]. Due to the more phosphoric acid uptake, it is not surprising that PBI/Im-$SiO_{3/2}$-X also shows higher conductivity than PBI/H_3PO_4/ZC-SiO_2 hybrid membranes in our previous work [13].

There are two mechanisms contribute the proton transfer in PEMs: Grotthuss mechanism and Vehicle mechanism [37]. It has been reported that the Grotthuss mechanism is the predominant mechanism for proton conduction for phosphoric acid doped membranes [36,38]. The activation energy (E_a) obtained from the proton conductivity of membranes is presented in Table 3. It can be seen that the E_a values are strongly related to the content of Im-$SiO_{3/2}$. For example, the phosphoric acid doped pure PBI membrane shows the highest E_a value but the lowest proton conductivity, which indicates that the proton transfer in the membrane needs more energy. In addition, the E_a values of the hybrid membranes in this work were comparable to that of other phosphoric acid doped membranes [31,36]. The prevailing mechanism for proton transport is often indicated by the slope of the Arrhenius plot of conductivity [39,40]. For all the samples, only PBI/Im-$SiO_{3/2}$-20 shows a small

Table 1
Mechanical properties of the acid-undoped and acid-doped membranes (Temp. 25 °C and 40–45% RH).

Membrane	Tensile strength (MPa)		Young's modulus (MPa)		Elongation at break (%)	
	Undoped	Doped	Undoped	Doped	Undoped	Doped
Pure PBI	56.33 ± 0.75	16.21 ± 1.09	1350 ± 230	326 ± 44	28.13 ± 1.12	124.65 ± 9.12
PBI/Im-$SiO_{3/2}$-5	58.31 ± 0.88	15.41 ± 0.64	1820 ± 170	297 ± 29	20.03 ± 2.13	76.65 ± 6.32
PBI/Im-$SiO_{3/2}$-10	60.62 ± 0.47	14.06 ± 0.76	2270 ± 290	316 ± 32	18.78 ± 2.35	84.65 ± 6.11
PBI/Im-$SiO_{3/2}$-15	63.81 ± 0.63	17.77 ± 1.45	2530 ± 310	365 ± 57	16.81 ± 1.67	72.65 ± 6.87
PBI/Im-$SiO_{3/2}$-20	66.51 ± 0.56	16.68 ± 0.94	2720 ± 130	302 ± 33	13.86 ± 2.06	68.65 ± 7.68

Table 2
Phosphoric acid doping capacity of PBI-based membranes.

Membrane	H_3PO_4 doping level (wt%)	H_3PO_4 doping level after water-extraction treatment (wt%)
Pure PBI	107	39.6
PBI/Im-$SiO_{3/2}$-5	120	62.5
PBI/Im-$SiO_{3/2}$-10	132	76.3
PBI/Im-$SiO_{3/2}$-15	147	96.6
PBI/Im-$SiO_{3/2}$-20	164	116.9

Table 3
Energy of activation (E_a) for phosphoric acid doped membranes.

Membrane	E_a (KJ mol^{-1})
Pure PBI	29.97
PBI/Im-$SiO_{3/2}$-5	25.54
PBI/Im-$SiO_{3/2}$-10	24.77
PBI/Im-$SiO_{3/2}$-15	24.55
PBI/Im-$SiO_{3/2}$-20	23.75
PA doped PBI/PVT [36]	20.27–26.45
PA doped imidazolium ionomers [31]	21.3–28.0

deviation from Arrhenius behavior at higher temperature (Fig 4). Compared with other membranes, there is more phosphoric acid in PBI/Im-$SiO_{3/2}$-20, the excess phosphoric acids in PBI/Im-$SiO_{3/2}$-20 act as concentrated phosphoric acid solution, and the self-diffusion of the excess phosphate moieties also contribute to proton transport (vehicle mechanism). Therefore, the proton transport behavior in the phosphoric acid doped hybrid membranes synthesized in this work also a combination of Grotthuss and vehicular mechanisms, and predominantly by the Grotthuss mechanism in the temperature range from 100 to 180 °C.

3.7. Retention ability of H_3PO_4

It is well to known that PA is a good proton carriers specially at elevated temperature. However, The long-term operation of the PA-doped PEMs could be affected by the progressive release of PA. In the present work, it is expected that the introduction of Im-$SiO_{3/2}$ could enhance the PA retention ability of the hybrid membranes. PA is water soluble, therefore, the retention ability of PA in the PBI-based membranes was confirmed by determining the weight loss of membrane samples after immersion in distilled water, and the values of H_3PO_4 doping level after water-extraction treatment were also listed in Table 2. It can be seen that the PA-doped pure PBI membrane loses about 70 wt% of their H_3PO_4 in 120 min (Fig 5). It is worth noting that H_3PO_4 retention ability of the hybrid membranes increased with the Im-$SiO_{3/2}$ content probably due to the interactions between H_3PO_4 and imidazolium groups (such as ionic or hydrogen bonding) [31], and more than 70 wt% H_3PO_4 is kept in the PBI/Im-$SiO_{3/2}$-20 hybrid membrane after being extracted with distilled water for 120 min. In the PBI/H_3PO_4/ZC-SiO_2 hybrid membranes, besides the ionic bond forces between the amino groups of the zwitterion-coated silica nanoparticles and H_3PO_4, the capillary forces among the silica nanospheres could also improve

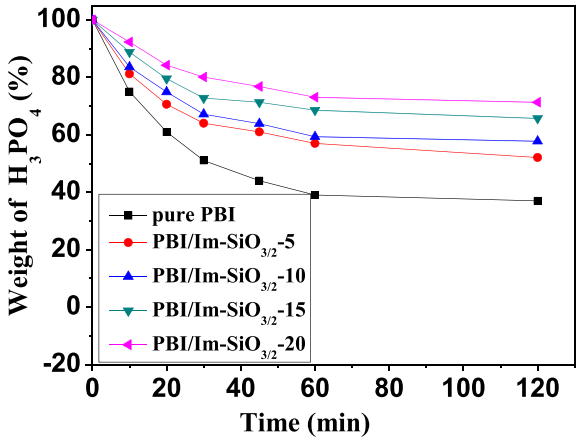

Fig. 5. Phosphoric acid retention ability test carried out in distilled water.

the H_3PO_4 retention ability [11,13]. Therefore, more H_3PO_4 was kept in PBI/H_3PO_4/ZC-SiO_2 hybrid membrane than that of PBI/Im-$SiO_{3/2}$-20 hybrid membrane in the present work after being extracted with distilled water.

The enhanced H_3PO_4 retention ability was further confirmed by the conductivity measurements of the water extracted PBI-based membranes. Fig. 6 shows that the conductivity of the PBI-based membranes was dramatically decreased after the extraction with water because of the high solubility of H_3PO_4 in water. The PBI/Im-$SiO_{3/2}$-20 membrane shows the highest conductivity compared to the plain and other PBI-based hybrid membranes. These results further confirmed the hybrid membranes are effective in holding H_3PO_4. Though there is less H_3PO_4 was kept in PBI/Im-$SiO_{3/2}$-15 (65.7 wt% of the total H_3PO_4 uptake) than that of PBI/H_3PO_4/ZC-

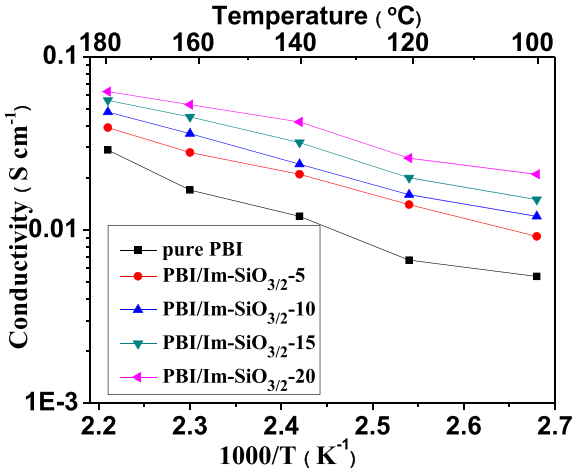

Fig. 4. Proton conductivity of PA-doped PBI-based membranes.

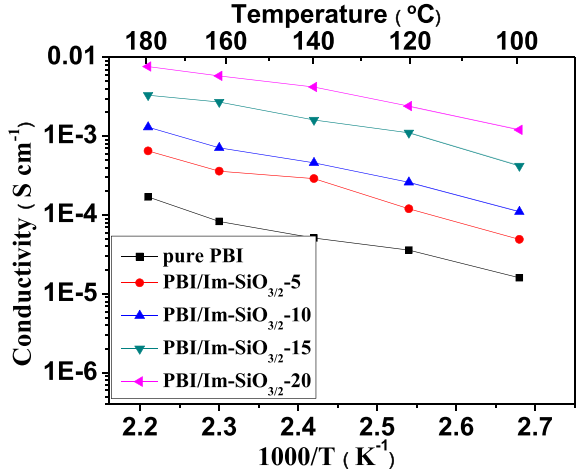

Fig. 6. Proton conductivity of PBI-based membranes after water-extraction treatment.

SiO_2-15 (79 wt% of the total H_3PO_4 uptake) [13] after the extraction with water for 120 min, PBI/Im-$SiO_{3/2}$-15 shows a little higher conductivity (2.7×10^{-3} S cm^{-1}, at 160 °C) than that of PBI/H_3PO_4/ZC-SiO_2-15 (2.3×10^{-3} S cm^{-1}, at 160 °C). This is probably due to smaller Im-$SiO_{3/2}$ was formed and more uniform distribution in membranes by sol–gel process than that of ZC-SiO_2 in PBI/H_3PO_4/ZC-SiO_2-15, which favors the formation of phosphoric acid continuous networks, and the proton conduction becomes more easy and feasible in PBI/Im-$SiO_{3/2}$-15.

4. Conclusion

In summary, PA-doped PBI/Im-$SiO_{3/2}$ hybrid membranes were synthesized and characterized, which show promise for use in high temperature PEMFCs. The interaction between imidazole groups on the surface of Im-$SiO_{3/2}$ and H_3PO_4 is favor of improving the acid uptake ability, which improve the proton conductivity of the hybrid membranes. The hybrid membranes were found to have good thermal stability up to 200 °C by TGA analysis, as well as high proton conductivities up to the order of 10^{-2} S cm^{-1} at 180 °C under anhydrous conditions. The proton conductivity of hybrid membranes increased with increasing the content of Im-$SiO_{3/2}$. Furthermore, the yielded hybrid membranes showed a better H_3PO_4 retention ability than the pure PBI membrane. These results prove that the PBI/Im-$SiO_{3/2}$ hybrid membrane has a strong potential for application in high temperature PEMFCs. The results of the study suggest a feasible approach for the synthesis and practical applications of this kind of proton exchange membranes.

Acknowledgments

This work was supported by National High Technology Research and Development Program 863 (2011AA050511), Natural Science Foundation of China (No. 51272033, 51303017 and 51342010).

References

[1] V. Di Noto, E. Negro, J.Y. Sanchez, C. Iojoiu, J. Am. Chem. Soc. 132 (2010) 2183–2195.
[2] S.S. Sekhon, J.S. Park, J.S. Baek, S.D. Yim, T.H. Yang, C.S. Kim, Chem. Mater. 22 (2010) 803–812.
[3] K.T. Adjemian, S. Lee, S. Srinivasan, J. Benziger, A.B. Bocarsly, J. Electrochem. Soc. 149A (2002) 256–261.
[4] S.I. Lee, K.H. Yoon, M. Song, H.G. Peng, K.A. Page, C.L. Soles, D.Y. Yoon, Chem. Mater. 24 (2012) 115–122.
[5] S. Bose, T. Kuila, T.X. Hien Nguyen, N.H. Kim, K. Lau, J.H. Lee, Prog. Polym. Sci. 36 (2011) 813–843.
[6] J.A. Asensio, E.M. Sanchez, P. Gomez-Romero, Chem. Soc. Rev. 39 (2010) 3210–3239.
[7] L.E. Karlsson, P. Jannasch, J. Membr. Sci. 230 (2004) 61–70.
[8] D.S. Kim, B. Liu, M.D. Guiver, Polymer 47 (2006) 7871–7880.
[9] T. Tezuka, K. Tadanaga, A. Hayashi, M. Tatsumisago, J. Am. Chem. Soc. 128 (2006) 16470–16471.
[10] M.L. Di Vona, E. Sgreccia, S. Licoccia, M. Khadhraoui, R. Denoyel, P. Knauth, Chem. Mater. 20 (2008) 4327–4334.
[11] B. Lin, S. Cheng, L. Qiu, F. Yan, S. Shang, J. Lu, Chem. Mater. 22 (2010) 1807–1813.
[12] Suryani, Y. Liu, J. Membr. Sci. 332 (2009) 121–128.
[13] F. Chu, B. Lin, B. Qiu, Z. Si, L. Qiu, Z. Gu, J. Ding, F. Yan, J. Lu, J. Mater. Chem. 22 (2012) 18411–18417.
[14] J. Zhu, G. Zhang, K. Shao, C. Zhao, H. Li, H. Na, J. Power Sources 196 (2011) 5803–5810.
[15] K.S. Roelofs, A. Kampa, T. Hirth, T.J. Schieste, Appl. Polym. Sci. 6 (2009) 2998–3009.
[16] Y. Zhou, W. Xiang, S. Chen, S. Fang, X. Zhou, J. Zhang, Y. Lin, Chem. Commun. (2009) 3895–3897.
[17] J. Kim, S. Mulmi, C. Lee, H. Park, Y. Chung, Y. Lee, J. Membr. Sci. 283 (2006) 172–181.
[18] M.L.D. Vona, Z. Ahmed, S. Bellitto, A. Lenci, E. Traversa, S. Licoccia, J. Membr. Sci. 296 (2007) 156–161.
[19] E.I. Santiago, R.A. Isidoro, M.A. Dresch, B.R. Matos, M. Linardi, F.C. Fonseca, Electrochim. Acta 54 (2009) 4111–4117.
[20] F. Yan, S. Yu, X. Zhang, L. Qiu, F. Chu, J. You, J. Lu, Chem. Mater. 21 (2009) 1480–1484.
[21] J. Weber, K.D. Kreuer, J. Maier, A. Thomas, Adv. Mater. 20 (2008) 2595–2598.
[22] T.L. Greaves, C.J. Drummond, Chem. Rev. 108 (2008) 206–237.
[23] S. Yi, F. Zhang, W. Li, C. Huang, H. Zhang, M. Pan, J. Membr. Sci. 366 (2011) 349–355.
[24] S.Y. Lee, A. Ogawa, M. Kanno, H. Nakamoto, T. Yasuda, M. Watanabe, J. Am. Chem. Soc. 132 (2010) 9764–9773.
[25] J.A. Asensio, P. Gómez-Romero, Fuel Cells 5 (2005) 336–343.
[26] J. Yang, Q. Li, J.O. Jensen, C. Pan, L.N. Cleemann, N.J. Bjerrua, R. He, J. Power Sources 205 (2012) 114–121.
[27] M. Schuster, T. Rager, A. Noda, K.D. Kreuer, J. Maier, Fuel Cells 5 (2005) 355–365.
[28] H. Steininger, M. Schuster, K.D. Kreuer, A. Kaltbeitzel, B. Bingol, W.H. Meyer, S. Schauff, G. Brunklaus, J. Maier, H.W. Spiess, Phys. Chem. Chem. Phys. 9 (2007) 1764–1773.
[29] H. Deligöz, M. Yılmazoğlu, J. Power Sources 196 (2011) 3496–3502.
[30] S.K. Kim, S.W. Choi, W.S. Jeon, J.O. Park, T. Ko, H. Chang, J.C. Lee, Macromolecules 45 (2012) 1438–1446.
[31] Z. Si, F. Gu, J. Guo, F. Yan, J. Polym. Sci. B. Polym. Phys. 51 (2013) 1311–1317.
[32] M. Litschauer, M.A. Neouze, J. Mater. Chem. 18 (2008) 640–646.
[33] S.W. Chuang, S.L.C. Hsu, J. Polym. Sci. A. Polym. Chem. 44 (2006) 4508–4513.
[34] Q. Li, H.C. Rudbeck, A. Chromik, J.O. Jensen, C. Pan, T. Steenberg, J. Membr. Sci. 347 (2010) 260–270.
[35] Y. Su, Y. Liu, Y. Sun, J. Lai, M. Guiver, Y. Gao, J. Power Sources 155 (2006) 111–117.
[36] M. Hazarika, T. Jana, ACS Appl. Mater. Interfaces 4 (2012) 5256–5265.
[37] H. Pu, W.H. Meyer, G. Wegmer, J. Polym. Sci. B. Polym. Phys. 40 (2002) 663–669.
[38] U.A. Rana, P.M. Bayley, R. Vijayaraghavan, P. Howlett, D.R. MacFarlane, M. Forsyth, Phys. Chem. Chem. Phys. 12 (2010) 11291–11298.
[39] H. Pei, L. Hong, J.Y. Lee, J. Power Sources 160 (2006) 949–956.
[40] B. Smitha, S. Sridhar, A.A. Khan, Macromolecules 37 (2004) 2233–2239.